Thermalization of free positronium atoms by collisions with silica-powder grains, aerogel grains, and gas molecules

Y. Nagashima, M. Kakimoto,* T. Hyodo, and K. Fujiwara†
Institute of Physics, College of Arts and Sciences, University of Tokyo, 3-8-1 Komaba, Meguro-ku, Tokyo 153, Japan

A. Ichimura
Institute of Space and Astronautical Science, 3-1-1 Yoshinodai, Sagamihara, Kanagawa 229, Japan

T. Chang and J. Deng
Institute of High Energy Physics, Academia Sinica, P. O. Box 2732, Beijing, China

T. Akahane and T. Chiba
National Institute for Research in Inorganic Materials, Namiki, Tsukuba, Ibaraki 305, Japan

K. Suzuki
Institute for Solid State Physics, University of Tokyo, 7-22-1, Roppongi, Minato-ku, Tokyo 106, Japan

B. T. A. McKee and A. T. Stewart
Department of Physics, Queen's University, Kingston, Ontario, Canada K7L 3N6
(Received 18 May 1994; revised manuscript received 28 February 1995)

Angular correlation of annihilation radiation (ACAR) from silica-powder pellets and silica aerogel has been measured in order to investigate the slowing down of free positronium (Ps) atoms by collisions with silica grains and gas molecules. The data for the pellets and the aerogel in vacuum show that the slowing down of parapositronium (p-Ps) in the free space between the silica grains depends on the number of collisions and hence on the mean distance between the grains. The momentum distribution of orthopositronium (o-Ps) shows further slowing down because of its long lifetime. From the ACAR data obtained from specimens of aerogel filled with gases (He, Ne, Ar, Kr, Xe, H_2, CH_4, CO_2, and iso-C_4H_{10}), the momentum-transfer cross sections between Ps and the gas molecules are estimated. It is concluded that the Ps kinetic energy is transferred only to the translational motion of the gas molecules, i.e., the excitations of vibration and rotation of the molecules are negligible.

PACS number(s): 36.10.Dr, 34.50.−s, 78.70.Bj

I. INTRODUCTION

It was observed in the mid 1960s that the angular correlation of annihilation radiation (ACAR) and positron lifetime spectra in metal oxide and metal fluoride powders [1,2] showed formation of positronium (Ps). In 1968, Paulin and Ambrosino [3] reported that the Ps component in the positron lifetime spectra for silica powders depends on the grain diameter. It was postulated that the Ps atoms form inside the grains and then diffuse out of them [4]. Paulin and Ambrosino also observed the effect of air on the o-Ps annihilation. Following this, silica powders were used for investigating the interactions between Ps and paramagnetic gases [5–8].

Chang *et al.* [9] reported in 1982 that silica aerogel showed a similar Ps formation property as powders. This material provides a convenient positron moderator, Ps formation medium, and "a microgas cell" for studies of Ps-gas scattering with the ACAR method [10,11]. The following points are to be emphasized. (i) The use of this special medium enables us to do ACAR measurements on dilute gases with much higher resolution without losing statistics than the "pure" gas experiments [12–14]. This is because the implantation depth of the ^{22}Na positrons into the aerogel of a typical density of 0.1 g/cm^3 is only 2.2 mm. Thus the region where the positrons annihilate is thin enough that the reduction of the count rate due to the sample collimator slit for the high resolution ACAR measurement is not serious [15]. (ii) The amount of Ps provided to the free space between the grains is large; the fraction of these Ps atoms is about 45% of the injected positrons for the aerogel with the grain diameter of 5 nm. (iii) Not only o-Ps but also parapositronium (p-Ps) is ejected out of the grain into the free space before annihilation [10]. This gives information on the momentum distribution at the time of the annihilation of p-Ps, on an average 125 ps after its formation. (iv) The momentum

*Present address: Information System Laboratory, Toshiba Research & Development Center, 1 Toshiba-cho, Komukai, Kawasaki, Kanagawa 210, Japan.
†Deceased.

distribution of o-Ps can be measured by applying a static magnetic field to induce it to annihilate into two γ rays. Note that the momentum distribution can be measured only through the γ rays from 2γ annihilation. (v) The mean lifetime of o-Ps can be controlled by changing the magnetic field.

The mean free path of the Ps in free space in the aerogel of grain diameter 5 nm and density 0.1 g/cm^3, as has been used in the present work as well as in Refs. [9,10,15–23], is long enough for the Ps atom in this space to be described as a free particle. The macroscopic structure of the aerogel is sustained by a delicate three-dimensional network even at this low density. Thus the aerogel can be handled—gently—just as a solid sample. The internal free space between the silica grains is connected to the space outside the aerogel because the aerogel is made from silica-methanol-gel by extracting water and methanol from the space between the grains [24,25]. Therefore, gas molecules are easily introduced into the free space by placing the aerogel in the gas atmosphere of desired pressure. Although the ACAR data obtained by using the aerogel include the component resulting from the positrons annihilating with the electrons of the silica grains, it is rather easy to subtract the component from the data.

Silica powders can be used in a way similar to the aerogel. An advantage of the powders is that we may change the mean distance between the grains by changing their packing. They can be pressed into pellets for high densities, but need special care for smaller densities.

The ACAR study with silica aerogel has already been applied to investigate the spin conversion collisions of Ps and oxygen [15,16] and the "anomalous" Ps formation fraction in Xe [18]. A number of other preliminary results have also been published [10,20,21,23].

In the present work, the ACAR method using silica aerogel is applied to a study of Ps slowing down through the collisions with various gas molecules. From the data, we estimate the momentum-transfer cross section between Ps and the gas molecules.

Prior to the gas experiments, the momentum distribution of p-Ps and o-Ps was measured by the ACAR method for the silica aerogel and pressed pellets of silica powders with different mean distances between the grains. The result is used to estimate the effect of the collisions with the grains in the analysis of the experiments with gases. Of course, the interaction of Ps with the silica grain surfaces is of interest for its own sake [26–31].

In Sec. II the experimental procedure is described. The experimental results are presented in Sec. III. In Sec. IV the p-Ps energy distribution is discussed, a model for the slowing down of Ps is presented, the effect of collisions with silica grain surfaces is discussed, and then the momentum-transfer cross sections are estimated.

II. EXPERIMENTAL PROCEDURE

The effect of collisions with the silica grains on the Ps momentum distribution in silica powders and silica aerogel was studied first. The powder (Cab-o-sil) having a mean diameter of 7 nm was pressed into pellets of macroscopic densities of 1.0 g/cm^3 and 0.3 g/cm^3. The macroscopic density of the silica aerogel was 0.1 g/cm^3. The mean grain diameter of the aerogel was measured to be 5 nm by using an electron microscopy and Brunauer-Emmett-Teller (BET) method. Two high resolution one-dimensional (1D) ACAR apparatuses were used; the one used for the measurements with the powder pellets was at Queen's University and the other used for the measurements with the aerogel was at University of Tokyo. The former was used with the momentum resolution 0.5×10^{-3} mc [full width at half maximum (FWHM)] and the latter with 0.27×10^{-3} mc (FWHM), where m and c are the electron mass and the light velocity, respectively. The powder pellets and the aerogel were placed in vacuum.

The ACAR for the aerogel in the presence of a static magnetic field of flux density 0.29 T was also measured. In the presence of a static magnetic field, the p-Ps state and one of the three substates of o-Ps are mixed to form two new well-defined quantum states that may self-annihilate into 2γ or 3γ [32]. We shall refer to them as para-like-positronium (p-like-Ps) and ortho-like-positronium (o-like-Ps) because in the limit of the field approaching zero, each converges to p-Ps and o-Ps, respectively. The mean lifetime of the p-like-Ps in the field of the present experiment is almost equal to that of p-Ps. On the other hand, that of the o-like-Ps is 51 ns. In the silica aerogel, the pickoff annihilation reduces this value to 49 ns [10].

The effects of the collisions of Ps with gas molecules were studied with the apparatus at University of Tokyo. Research grade high purity gaseous He, Ne, Ar, Kr, Xe, H_2, CH_4, iso-C_4H_{10}, and CO_2 were introduced into the free space between the grains of the silica aerogel by filling the sample chamber with these gases. The pressure of the gases was 1 atm. ACAR data were obtained with and without the static magnetic field of 0.29 T. The pickoff annihilation with the gas molecules further reduces the mean lifetime of the o-like-Ps by up to 2 ns [33]. All the measurements were performed at room temperature.

III. RESULTS

A. Data in vacuum

Figure 1 shows the ACAR data for (a) the silica aerogel (0.1 g/cm^3), (b) the powder pellet of density 0.3 g/cm^3, (c) the powder pellet of density 1.0 g/cm^3, and (d) the silica aerogel in the magnetic field. The solid curves show the same Gaussian curve with a FWHM of 10.0×10^{-3} mc (broad components), which has been determined by fitting to the data points in the region $|p_z| > 5 \times 10^{-3}$ mc. These represent the momentum distributions of the valence and the inner core electrons in fused silica sampled by the positrons. The ACAR data in Fig. 1 are normalized to the same broad component intensities. The narrower component in Figs. 1(a)–1(c) represents the momentum distribution of p-Ps in the free space be-
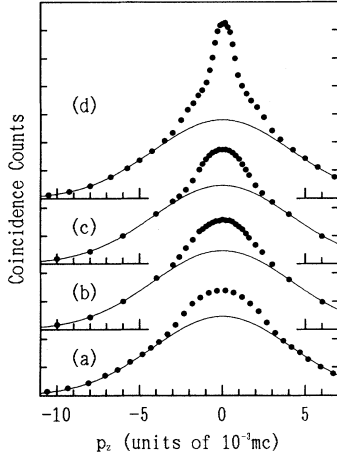
FIG. 1. ACAR data for (a) the silica aerogel (0.1 g/cm^3), (b) the powder pellet of density 0.3 g/cm^3, (c) the powder pellet of density 1.0 g/cm^3, all in zero field, and (d) the silica aerogel in the magnetic field of 0.29 T. The solid curves show the broad component.

tween the silica grains. The data in Fig. 1(d) contain an additional narrowest component that comes from the 2γ self-annihilation of o-like-Ps induced by the magnetic field. Figures 2(a)–2(c) show the momentum distribution $N(p_z)$ of the p-Ps obtained by subtracting the solid curves from the data shown in Fig. 1. Figure 2(d) shows the momentum distribution of the o-like-Ps obtained by subtracting Fig. 1(a) from 1(d).

In order to correct for the effect of the experimental resolution, $N(p_z)$, shown in Fig. 2, was decomposed into two or three Gaussians. Then the resolution was deconvoluted quadratically.

The average energy $\varepsilon_{\mathrm{av}}^{\mathrm{obs}}$ of the p- and o-like-Ps is calculated from $N(p_z)$ by

$$\varepsilon_{\mathrm{av}}^{\mathrm{obs}}(\tau) = 3 \int_{-\infty}^{\infty} \frac{p_z^2}{2m_{\mathrm{Ps}}} N(p_z) dp_z \Big/ \int_{-\infty}^{\infty} N(p_z) dp_z, \quad (1)$$
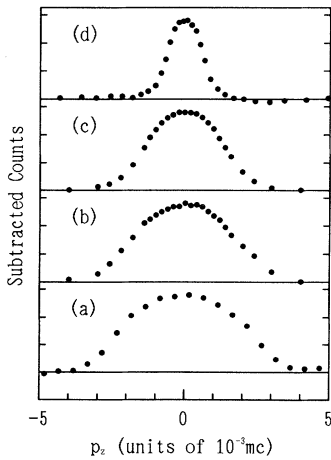

FIG. 2. (a)–(c) p-Ps momentum distributions obtained by subtracting the solid curves from Figs. 1(a)–1(c). (d) o-like-Ps momentum distribution obtained by subtracting Fig. 1(a) from Fig. 1(d).
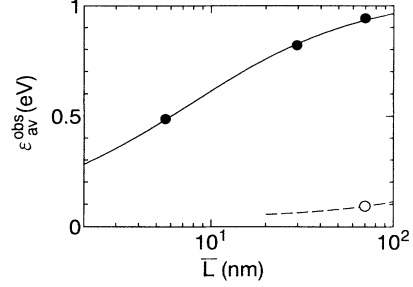

FIG. 3. Average energy $\varepsilon_{\mathrm{av}}^{\mathrm{obs}}$ of p-Ps (full circles) and o-like-Ps (open circle). The solid line represents $\varepsilon_{\mathrm{av}}^{(2)}(\tau)$ with $\overline{M_s} = 13$ amu for p-Ps, while the dashed line represents $\varepsilon_{\mathrm{av}}^{(2)}(\tau)$ with $\overline{M_s} = 23$ amu for o-like-Ps.

where m_{Ps} is the Ps mass and τ is the mean lifetime of the Ps. In Fig. 3, $\varepsilon_{\mathrm{av}}^{\mathrm{obs}}(\tau)$ is plotted against the mean distance $\overline{L}$ between the grains. $\overline{L}$ has been calculated with the assumption of uniform size and spatial distributions of the grains as

$$\overline{L} = \frac{4}{3} \left(\frac{\rho_0}{\rho} - 1 \right) R, \quad (2)$$

where ρ_0 is the bulk density of amorphous silica (2.20 g/cm^3), ρ is the density of the aerogel or the powder pellets, and R is the mean radius of the grains.

B. Data in the presence of gases

Figure 4 shows the ACAR data taken with the silica aerogel placed in gases at a pressure of 1 atm (10^5 Pa) in zero field, while Fig. 5 shows those in the field of 0.29 T. The ACAR curves are normalized to the same broad component (solid curve) intensities. For Kr and Xe, the peak values are higher than those for the other gases and vacuum. This is due to the efficient formation of Ps on collisions with the heavier inert gas molecules [18]. Figure
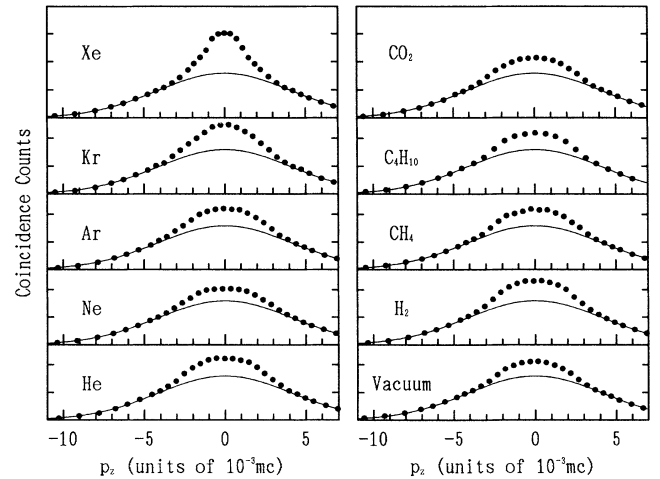

FIG. 4. ACAR data for silica aerogel in gases in zero field. The solid curves show the broad component.

THERMALIZATION OF FREE POSITRONIUM ATOMS BY ...

TABLE I. Average energy of the observed o-like-Ps components (ε_{av}^{obs}), the Ps momentum-transfer cross section ($\sigma_m^{(2)}$), and the total scattering cross section estimated by viscosity measurements (σ_{visc}). The value of $\sigma_m^{(2)}$ should be regarded as the upper limit (see text). The quantity $\sigma_m^{(2)}/M$, where M denotes the mass of the gas molecule, is a measure of relative thermalization rate. The value of $\sigma_m^{(1)}$ obtained by a different approximation described in the text is also listed for reference.

Gas	ε_{av}^{obs} (eV)	$\sigma_m^{(2)}$ (10^{-16} cm^2)	σ_{visc} (10^{-16} cm^2)	$\sigma_m^{(2)}/\sigma_{visc}$	$\sigma_m^{(2)}/M$ (10^{-16} cm^2/amu)	$(\sigma_m^{(1)})$ (10^{-16} cm^2)
vacuum	0.093					
He	0.051	52	8.2	6.3	13	(2.0)
Ne	0.070	60	10	6.0	3.0	(3.7)
Ar	0.082	63	17	3.7	1.6	(3.6)
Kr	0.088	61	21	2.9	0.73	(3.8)
Xe	0.072	1.2×10^2	27	4.4	0.91	(17)
H_2	0.046	48	11	4.4	24	(1.3)
CH_4	0.063	69	21	3.3	4.3	(4.3)
iso-C_4H_{10}	0.067	1.6×10^2	49	3.3	3.6	(12)
CO_2	0.071	1.3×10^2	25	5.2	2.2	(8.1)

6 shows the o-like-Ps momentum distribution obtained by subtracting the zero-field data (Fig. 4) from the data in the field (Fig. 5). The ε_{av}^{obs} for the o-like-Ps obtained by using Eq. (1) are listed in Table I.

IV. DISCUSSION

A. Energy distribution of p-Ps

The p-Ps average energy deduced from Figs. 2(a)–2(c) is shown in Fig. 3. It depends on the mean distance between the silica grains. This confirms that Figs. 2(a)–2(c) are not due to the p-Ps atoms in the grain or on the grain surface but those in the free space between the grains.

The Ps momentum density distribution $\rho(p)$ can be deduced from the component $N(p_z)$ in the 1D ACAR as [34]

$$\rho(p) \propto -\frac{1}{p_z}\frac{d}{dp_z}N(p_z)|_{p_z=p}. \tag{3}$$

Then, the corresponding Ps energy distribution is given by

$$f(E)dE \propto \sqrt{E}\, \rho(\sqrt{2m_{Ps}E})dE. \tag{4}$$

Figure 7 shows the energy distribution calculated from the p-Ps component shown in Fig. 2(a) using Eq. (4). It can be seen from the figure that energy distribution of Ps with the mean lifetime 125 ps has a peak at $E = 0.8$ eV.

The Ps kinetic energy lost per collision with an atom in silica powder is approximately $10^{-4}E$ [27] and the number of collisions in the present aerogel during the short lifetime of p-Ps is a few hundreds. The part of the energy lost before p-Ps annihilation is therefore only a few percent of the initial energy. If there is no other energy loss mechanism, it may be concluded that the energy of
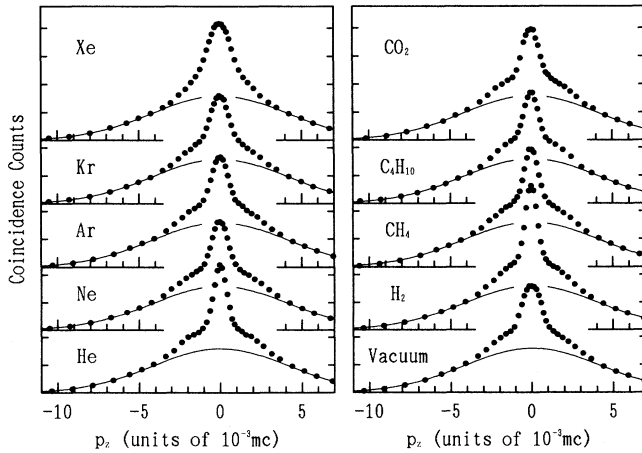

FIG. 5. ACAR data for silica aerogel in gases in the presence of a magnetic field of 0.29 T. The solid curves show the broad component.
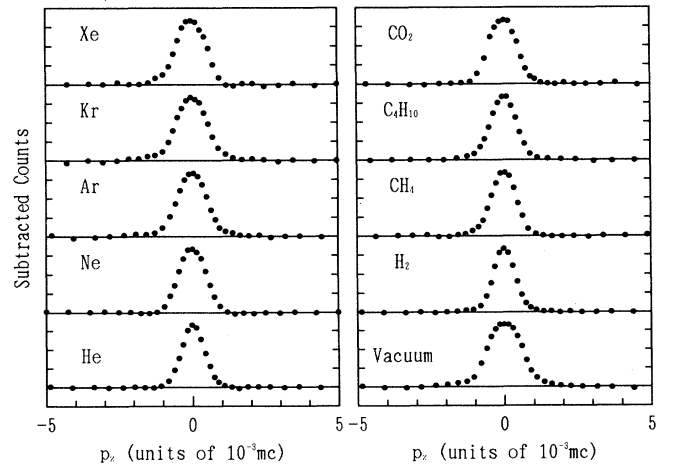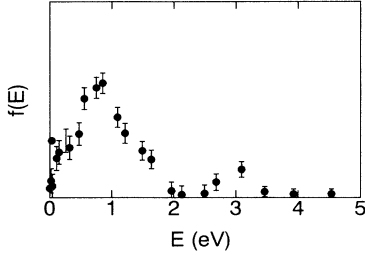

FIG. 6. o-like-Ps momentum distributions obtained by subtracting the zero-field data (Fig. 4) from the data in the field (Fig. 5).

FIG. 7. Energy distribution of p-Ps $f(E)$.

the Ps atoms emitted from the grain surfaces is approximately 0.8 eV. This value is the same as the effective potential barrier of the silica surface for Ps estimated by Fox and Canter [28]. However, the value is considerably smaller than that of the Ps work function for crystalline quartz (-3.27 eV) obtained in a direct measurement by Sferlazzo *et al.* [35] using a monoenergetic positron beam. The reason for this discrepancy is unknown. Although a small peak is seen at $E = 3$ eV in Fig. 7, it is difficult to conclusively relate with the observation of Sferlazzo *et al.* because it resulted from a small structure in the ACAR data at around 5×10^{-3} mc in Fig. 2(a).

B. Model for Ps energy loss

We must develop an expression for the time dependence of the average momentum of Ps interacting with gas molecules. Let a Ps atom of velocity v elastically collide with a molecule (mass M) of velocity V. The energy loss of the Ps atom averaged over the scattering angle (denoted by an overbar) and over the thermal distribution of the molecules (denoted by angular brackets) is given by [36]

$$-\langle \overline{\Delta E} \rangle = \frac{2m_{\mathrm{Ps}}M}{(m_{\mathrm{Ps}} + M)^2} \left(\frac{m_{\mathrm{Ps}}v^2}{2} - \frac{M\langle V^2 \rangle}{2} \right) \frac{\sigma_m}{\sigma_{\mathrm{tot}}}, \quad (5)$$

where

$$\sigma_m = 2\pi \int_0^\pi (1 - \cos\theta)\sigma(\theta)\sin\theta d\theta \quad (6)$$

is the momentum-transfer cross section and

$$\sigma_{\mathrm{tot}} = 2\pi \int_0^\pi \sigma(\theta)\sin\theta d\theta \quad (7)$$

is the total cross section for the elastic scattering with $\sigma(\theta)$ being the differential cross section.

We assume that σ_m and σ_{tot} are independent of the Ps energy and that the time derivative of the averaged Ps kinetic energy

$$E_{\mathrm{av}} = \left\langle \frac{m_{\mathrm{Ps}}v^2}{2} \right\rangle = \frac{m_{\mathrm{Ps}}v_{\mathrm{rms}}^2}{2}$$

is described by

$$\frac{dE_{\mathrm{av}}}{dt} \approx \langle \overline{\Delta E} \rangle f_{\mathrm{coll}}$$

$$\approx \langle \overline{\Delta E} \rangle v_{\mathrm{rms}} \sigma_{\mathrm{tot}} n, \quad (8)$$

where f_{coll} is the collision frequency and n is the number density of the gas molecules. The averaged velocity of the Ps is approximated by root-mean-square velocity v_{rms} of Ps. Then we get the differential equation

$$\frac{dE_{\mathrm{av}}(t)}{dt} = -\frac{2\sigma_m n}{M}\sqrt{2m_{\mathrm{Ps}}E_{\mathrm{av}}(t)}(E_{\mathrm{av}}(t) - \tfrac{3}{2}k_B T), \quad (9)$$

where we have set $M\langle V^2 \rangle/2 = (3/2)k_B T$. The approximation that $M + m_{\mathrm{Ps}} \approx M$ has been used. Equation (9) can be easily solved as

$$E_{\mathrm{av}}(t) = \left(\frac{1 + Ae^{-bt}}{1 - Ae^{-bt}} \right)^2 \frac{3}{2}k_B T, \quad (10)$$

where

$$b = \frac{2\sigma_m n}{M}\sqrt{3m_{\mathrm{Ps}}k_B T} \quad (11)$$

and A is a constant determined by the initial condition; if the average Ps energy at $t = 0$ is E_0, then

$$A = \frac{\sqrt{E_0} - \sqrt{\tfrac{3}{2}k_B T}}{\sqrt{E_0} + \sqrt{\tfrac{3}{2}k_B T}}. \quad (12)$$

Now we further assume that the Ps energy loss process due to the collisions with the silica grain surface may also be described by Eq. (8) with the average energy loss on collision (5) replaced by

$$-\langle \overline{\Delta E} \rangle = \frac{2m_{\mathrm{Ps}}}{\overline{M_s}} \left(\frac{m_{\mathrm{Ps}}v^2}{2} - \frac{3}{2}k_B T \right) \quad (13)$$

and the collision frequency by $v_{\mathrm{rms}}/\overline{L}$. Here $\overline{M_s}$ is the effective mass of the surface atoms and $\overline{L}$ is the mean distance between the grains. If we assume that $\overline{M_s}$ and σ_m are independent of the Ps energy, the average energy of Ps in the presence of both silica grains and gas molecules are given by Eq. (10) with

$$b = \left(\frac{2\sigma_m n}{M} + s \right)\sqrt{3m_{\mathrm{Ps}}k_B T}, \quad (14)$$

where we have introduced

$$s = \frac{2}{\overline{L}\,\overline{M_s}}, \quad (15)$$

which represents the effect of the collisions with the surface.

Strictly, we should take the Ps velocity distribution into consideration in these derivations. Such an approach based on the Boltzmann equation will be discussed elsewhere. The resulting formula for Ps thermalization is not so different from the above model.

Equation (10) represents the average Ps energy at time t. The average Ps energy $\varepsilon_{\mathrm{av}}^{\mathrm{obs}}(\tau)$ deduced from the ACAR data by using Eq. (1) is, on the other hand, that
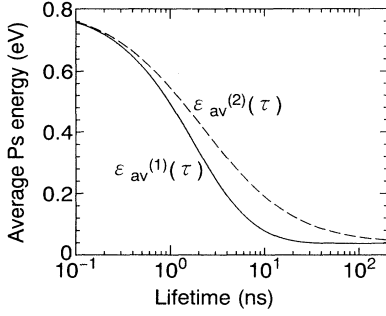
FIG. 8. Average Ps energy $\varepsilon_{\text{av}}^{(1)}(\tau)$ (solid curve) and $\varepsilon_{\text{av}}^{(2)}(\tau)$ (broken curve) calculated for the case $b = 1.3 \times 10^8$ s^{-1}.

for Ps atoms with the mean lifetime τ averaged over time from $t = 0$ to ∞. A simplest approach to relate these is to compare $\varepsilon_{\text{av}}^{\text{obs}}(\tau)$ to a "typical" energy

$$\varepsilon_{\text{av}}^{(1)}(\tau) = E_{\text{av}}(\tau), \tag{16}$$

where E_{av} is given by Eq. (10) [11,20,21]. Sauder [36] estimated the lower limit of the thermalization time of Ps in Ar gas by comparing this with $\varepsilon_{\text{av}}^{\text{obs}}(\tau)$ obtained in the ACAR measurement for high pressure Ar gas. However, it is more appropriate to compare $\varepsilon_{\text{av}}^{\text{obs}}(\tau)$ with

$$\varepsilon_{\text{av}}^{(2)}(\tau) = \frac{1}{\tau} \int_0^\infty E_{\text{av}}(t) e^{-t/\tau} dt$$
$$= \left(1 + \sum_{k=1}^\infty \frac{4kA^k}{1 + b\tau k}\right) \frac{3}{2} k_B T. \tag{17}$$

The two different energies $\varepsilon_{\text{av}}^{(1)}(\tau)$ and $\varepsilon_{\text{av}}^{(2)}(\tau)$ are shown vs τ in Fig. 8 for the case $b = 1.3 \times 10^8$ s^{-1} (corresponding to $\overline{M_s} = 20$ amu if $n = 0$). The difference is substantial and thus $\varepsilon_{\text{av}}^{(1)}(\tau)$ can hardly be regarded as a good approximation to $\varepsilon_{\text{av}}^{(2)}(\tau)$.

C. Analysis of collisions with grain surface

The solid curve in Fig. 3 shows the result of fitting $\varepsilon_{\text{av}}^{(2)}(125\text{ ps})$ with $n = 0$ (vacuum) to $\varepsilon_{\text{av}}^{\text{obs}}$ for p-Ps in three different mean distances in two silica powder specimens and one silica aerogel specimen. The optimized value of $\overline{M_s}$ in Eq. (15) is 13 amu. The dashed curve shows the result of fitting $\varepsilon_{\text{av}}^{(2)}(49\text{ ns})$ to $\varepsilon_{\text{av}}^{\text{obs}}$ for o-like-Ps in silica aerogel. The optimized value for $\overline{M_s}$ is 23 amu. In the latter fitting we assumed that the parameter A in Eq. (17) is equal to the value obtained in the former fitting.

If we fit $\varepsilon_{\text{av}}^{(1)}(\tau)$ to the data, the optimized values of $\overline{M_s}$ are 22 amu for p-Ps and 112 amu for o-like-Ps. The reason that the analysis using $\varepsilon_{\text{av}}^{(1)}(\tau)$ gives a larger $\overline{M_s}$ can be understood from Fig. 8 which shows that $\varepsilon_{\text{av}}^{(1)}$ is smaller than $\varepsilon_{\text{av}}^{(2)}$ for the same τ.

In both cases, $\overline{M_s}$ for p-Ps is smaller than that for o-like-Ps. This indicates that the energy transfer to sil-

ica per collision becomes more difficult as the Ps kinetic energy gets lower [29].

D. Analysis of collisions with gas molecules

The momentum-transfer cross section σ_m between Ps and the gas molecule was estimated by comparing $\varepsilon_{\text{av}}^{(2)}(\tau)$ with $\varepsilon_{\text{av}}^{\text{obs}}$, where τ is the mean lifetime of the Ps including the effect of the pickoff annihilation with the gas molecules. We determined the two parameters A and b by solving the simultaneous equations of the type (17) for $\varepsilon_{\text{av}}^{(2)}$ ($\tau = 125$ ps) (p-Ps) and $\varepsilon_{\text{av}}^{(2)}$ ($\tau \sim 50$ ns) (o-like-Ps) numerically. For $\overline{M_s}$, which represents the effect of collisions with the silica grains, we used the value for o-like-Ps in the silica aerogel in vacuum (23 amu). The values for the momentum-transfer cross section $\sigma_m^{(2)}$ thus obtained are listed in Table I. The values estimated using $\varepsilon_{\text{av}}^{(1)}(\tau)$ and $\overline{M_s} = 112$ amu are also listed for reference (denoted by $\sigma_m^{(1)}$).

The cross section $\sigma_m^{(2)}$ is more meaningful than $\sigma_m^{(1)}$, since $\varepsilon_{\text{av}}^{(2)}$ is defined through realistic averaging. However, the values for $\sigma_m^{(2)}$ should be regarded as upper limits because we have assumed, for the sake of simplicity, that $\overline{M_s}$ is independent of the Ps energy in spite of the energy dependence of $\overline{M_s}$, as discussed in Sec. IV C. More reliable values of the cross section can be obtained through measurements with varying the lifetime of o-like-Ps by changing the magnetic flux density. However, such a series of the measurements takes long time and will be included in the subject on the next stage of our work. (Preliminary results for He have been reported in Ref. [23].)

In the present analysis, the scattering between Ps and gas molecules is assumed to be elastic. This assumption should be valid for inert gases. It is known that in the case of electron-molecule collisions the electron energy loss per collision is much larger for molecular gases than inert gases [39]. This is because the electron excites the vibrations or rotations of the polyatomic molecules. If this is also the case for Ps-molecular gas collisions, the above analysis, which takes only the elastic collision into account, would result in abnormally large "effective" cross sections for molecular gases. To check this, we compare our deduced cross sections with the "geometrical" cross sections

$$\sigma_{\text{visc}} = \pi (r_{\text{molec}}^{\text{visc}} + r_{\text{Ps}})^2, \tag{18}$$

where $r_{\text{molec}}^{\text{visc}}$ is the radius of the molecules estimated from the viscosity measurements [38] and r_{Ps} is the radius of Ps, which is taken to be the same as Bohr radius of the hydrogen atom. (Note that the center of mass of Ps is located midway between the electron and the positron.) The ratios $\sigma_m^{(2)}/\sigma_{\text{visc}}$ are also listed. No tendency is seen that the ratios for the molecular gases are larger than those for the inert gases. This shows that the scattering is essentially elastic for molecular gases too. This is in accord with the following simple consideration.

For an internal level of energy $h\nu$ of a gas molecule to

be effectively excited by the Ps impact, the interaction time τ_{int} must be on the same order of magnitude as the period ν^{-1}. Since both the Ps and the molecule are neutral, the interaction is van der Waals type and significant only when they come close to each other. Thus τ_{int} is given by

$$\tau_{int} \sim d_{mol}/v, \qquad (19)$$

where d_{mol} is the molecular diameter and v is the speed of the Ps. On the other hand, since Ps must have kinetic energy at least as large as $h\nu$ to excite the mode, v must satisfy

$$v \geq \sqrt{2h\nu/m_{Ps}}. \qquad (20)$$

Rotational states are separated typically by 10^{-3} eV. The interaction time of the Ps having sufficient kinetic energy to excite the modes of a molecule of size a_0 (Bohr radius) is therefore $\tau_{int} \leq 4 \times 10^{-15}$ s. This is much shorter than the corresponding rotational period of $\nu^{-1} \sim 4 \times 10^{-12}$ s. In addition, in the case of vibrational excitation of typical energy 0.1 eV, $\tau_{int} \leq 4 \times 10^{-16}$ s is much shorter than the corresponding vibrational period of $\nu^{-1} \sim 4 \times 10^{-14}$ s. This is in contrast to the case of electron scattering with molecules, where the range of the dipole interaction is much longer than the sizes of the molecules.

We list in Table I $\sigma_m^{(2)}/M$ as a measure for relative thermalization rate where M is the mass of the gas molecule. These values are consistent with the recent observation by Westbrook *et al.* [39], who found that the rate of Ps thermalization in iso-C_4H_{10} is similar to Ne, in contradiction to their initial expectation. Our data indicate that the thermalization in He and H_2 gas is considerably faster than that in iso-C_4H_{10}. Thus He and H_2 are more suitable for quick thermalization of Ps than iso-C_4H_{10}.

Several authors have measured the total scattering cross section, which should be close to the momentum-transfer cross section at low energy. In 1975, Spektor and Paul [40] estimated the total scattering cross sections for Ps in He, Ne, Ar, Kr, Xe, N_2, and iso-C_4H_{10} gases by studying the diffusion of Ps with the positron lifetime measurement. The obtained cross sections are three orders of magnitude smaller than our values of $\sigma_m^{(2)}$. Recently, Zafar *et al.* [41] estimated the total cross sections for He and Ar to be $(1.8–2.8)\times10^{-16}$ cm^2 and $(4.5–7.6)\times10^{-16}$ cm^2, respectively, in the $7 - 41$ eV Ps energy range by using Ps beam technique. They further made the first direct Ps beam measurement for Ar in the energy

range between 10 eV and 70 eV and obtained revised values that range from 8.9×10^{-16} cm^2 to 14.6×10^{-16} cm^2 [42]. Coleman *et al.* [14] estimated the Ps-atom scattering cross section from two-dimensional ACAR measurement for He, Ne, and Ar using the gases themselves as Ps formation media. Their estimation gives about 8×10^{-16} cm^2 for thermal Ps for all the gases. These values lie within our upper limit values.

Theoretical investigations have been also performed for He and H_2. For He, Fraser *et al.* [43] and Barker and Bransden [44] reported their calculated momentum-transfer cross sections at the Ps energy of 0.272 eV to be 10.6×10^{-16} cm^2 and 8.25×10^{-16} cm^2 respectively. Drachman and Houston [45] and Peach [46] reported the total scattering cross section at the Ps energy of 0 eV to be 6.8×10^{-16} cm^2 and 1×10^{-16} cm^2, respectively. In order to examine these values, more precise meaurement is necessary. For H_2, Comi *et al.* [47] calculated the total scattering cross section to be 149.4×10^{-16} cm^2. Our results suggest that this is too large.

V. CONCLUSIONS

We performed ACAR studies of thermalization for Ps-silica grain surface collisions and the momentum-transfer cross section for the Ps-gas molecule collisions. Silica powders and silica aerogel were used to form Ps. The Ps energy transfer to silica per collision becomes more difficult as the Ps kinetic energy gets lower. The estimated momentum-transfer cross sections for He, Ne, Ar, Kr, Xe, H_2, CH_4, iso-C_4H_{10}, and CO_2 are listed in Table I. These values should be regarded as upper limits of the cross section. They show that the Ps energy is transferred only to the translational motion of the gas molecules, i.e., the excitation of vibration and rotation of the molecules are negligible. As a consequence, Ps thermalization is considerably faster in He and H_2 than in other gases.

ACKNOWLEDGMENTS

[1] J. H. Kusmiss and A. T. Stewart, in *Positron Annihilation*, edited by A. T. Stewart and L. O. Roellig (Academic, New York, 1967), p. 341.

[2] R. Paulin and G. Ambrosino, in *Positron Annihilation* (Ref. [1]), p. 345.

[3] R. Paulin and G. Ambrosino, J. Phys. (Paris) **29**, 263 (1968).

[4] W. Brandt and R. Paulin, Phys. Rev. Lett. **21**, 193 (1968).

[5] P. Sen and A. P. Patro, Nuovo Cimento B **64**, 324 (1969).

[6] G. M. Bartenev, A. Z. Varisov, V. I. Gol'danskii, B. M. Levin, A. D. Mokrushin, and A. D. Tsyganov, Fiz. Tverd. Tela **11**, 3177 (1969) [Sov. Phys. Solid State **11**, 2575 (1970)].

[7] F. R. Steldt and P. G. Varlashkin, Phys. Rev. B **5**, 4265 (1972).

[8] V. I. Goldanskii, A. D. Mokrushin, A. O. Tatur, and V. P. Shantarovich, Appl. Phys. **5**, 379 (1975).

[9] T. B. Chang, Y. Y. Wang, C. C. Chang, and S. Wang, in *Positron Annihilation*, edited by P. G. Coleman, S. C. Sharma, and L. M. Diana (North-Holland, Amsterdam, 1982), p. 696.

[10] T. B. Chang, J. K. Deng, T. Akahane, T. Chiba, M. Kakimoto, and T. Hyodo, in *Positron Annihilation*, edited by P. C. Jain, R. M. Singru, and K. P. Gopinathan (World Scientific, Singapore, 1985), p. 974.

[11] T. Hyodo, in *Positron Annihilation*, edited by Zs. Kajcsos and Cs. Szeles, Materials Science Forum Vols. 105–110 (Trans Tech, Aedermannsdorf, 1992), p. 281.

[12] L. A. Page and M. Heinberg, Phys. Rev. **106**, 1220 (1957).

[13] M. Heinberg and L. A. Page, Phys. Rev. **107**, 1589 (1957).

[14] P. G. Coleman, S. Rayner, F. M. Jacobsen, M. Charlton, and R. N. West, J. Phys. B **27**, 981 (1994).

[15] M. Kakimoto, T. Hyodo, T. Chiba, T. Akahane, and T. B. Chang, J. Phys. B **20**, L107 (1987).

[16] M. Kakimoto, T. Hyodo, and T. B. Chang, J. Phys. B **23**, 589 (1990).

[17] T. Chang, M. Xu, and X. Zeng, Phys. Lett. A **126**, 189 (1987).

[18] M. Kakimoto and T. Hyodo, J. Phys. B **21**, 2977 (1988).

[19] T. Chang, in *Positron Annihilation*, edited by L. Dorikens-Vanpraet, M. Dorikens, and D. Segers (World-Scientific, Singapore, 1989), p. 150.

[20] M. Kakimoto, Y. Nagashima, T. Hyodo, K. Fujiwara, and T. B. Chang, in *Positron Annihilation* (Ref. [19]), p. 737.

[21] T. Hyodo, M. Kakimoto, T. B. Chang, J. Deng, T. Akahane, T. Chiba, B. T. A. McKee, and A. T. Stewart, in *Positron Annihilation* (Ref. [19]), p. 878.

[22] T. B. Chang, G. M. Yang, and T. Hyodo, in *Positron Annihilation* (Ref. [11]), p. 1509.

[23] Y. Nagashima, T. Hyodo, and K. Fujiwara, in *Positron Annihilation* (Ref. [11]), p. 1671.

[24] S. Henning and L. Svensson, Phys. Scr. **23**, 697 (1981).

[25] G. Poelz and R. Riethmüller, Nucl. Instrum. Methods **195**, 491 (1982).

[26] D. W. Gidley, K. A. Marko, and A. Rich, Phys. Rev. Lett. **36**, 395 (1976).

[27] G. W. Ford, L. M. Sander, and T. A. Witten, Phys. Rev. Lett. **36**, 1269 (1976).

[28] R. A. Fox and K. F. Canter, J. Phys. B **11**, L255 (1978).

[29] A. P. Mills, Jr., E. D. Shaw, R. J. Chichester, and D. M. Zuckerman, Phys. Rev. B **40**, 2045 (1989).

[30] F. A. Khangi, P. Rice-Evans, and D. L. Smith, in *Positron Annihilation* (Ref. [11]), p. 1371.

[31] C. E. Haynes, P. C. Rice-Evans, and F. A. R. El Khangi, J. Phys. Condens. Matter **6**, 2277 (1994).

[32] O. Halpern, Phys. Rev. **94**, 904 (1954).

[33] M. Charlton, Rep. Prog. Phys. **48**, 737 (1985).

[34] A. T. Stewart, Can. J. Phys. **35**, 168 (1957).

[35] P. Sferlazzo, S. Berko, and K. F. Canter, Phys. Rev. B **35**, 5315 (1987).

[36] W. C. Sauder, J. Res. Natl. Bur. Stand. **72A**, 91 (1968).

[37] L. G. Christophorou and J. G. Carter, Chem. Phys. Lett. **2**, 607 (1968).

[38] J. O. Hirschfelder, C. F. Curtiss, and R. B. Bird, *Molecular Theory of Gases and Liquids* (Wiley, New York, 1954).

[39] C. I. Westbrook, D. W. Gidley, R. S. Conti, and A. Rich, Phys. Rev. A **40**, 5489 (1989).

[40] D. M. Spektor and D. A. L. Paul, Can. J. Phys. **53**, 13 (1975).

[41] N. Zafar, G. Laricchia, M. Charlton, and T. C. Griffith, J. Phys. B **24**, 4661 (1991).

[42] N. Zafar, G. Laricchia, and M. Charlton, Hyp. Int. **89**, 243 (1994).

[43] P. A. Fraser, Proc. Phys. Soc. **79**, 721 (1961); P. A. Fraser and M. Kraidy, *ibid.* **89**, 533 (1966); P. A. Fraser, J. Phys. B **1**, 1006 (1968).

[44] M. I. Barker and B. H. Bransden, J. Phys. B **1**, 1109 (1968); **2**, 730 (1969).

[45] R. J. Drachman and S. K. Houston, J. Phys. B **3**, 1657 (1970).

[46] G. Peach, private communication.

[47] M. Comi, G. M. Prosperi, and A. Zecca, Phys. Lett. **93A**, 289 (1983); Nuovo Cimento **2**, 1347 (1983).